Advances in Multiresolution for Geometric Modelling,
N. A. Dodgson, M. S. Floater, M. A. Sabin (editors),
Springer, 2005, ISBN 3-540-21462-3, pp.285–299

$\sqrt{5}$-subdivision

Ioannis P. Ivrissimtzis[1], Neil A. Dodgson[2], and Malcolm Sabin[3]

[1] Max-Planck-Institut für Informatik, Saarbrücken, Germany
ivrissim@mpi-sb.mpg.de
[2] Computer Laboratory, University of Cambridge, UK
nad@cl.cam.ac.uk
[3] Numerical Geometry Ltd., Cambridge, UK
malcolm@geometry.demon.co.uk

Summary. Most established subdivision schemes have the refined grid at each stage aligned with the previous one. The $\sqrt{3}$ and $\sqrt{2}$ schemes alternate orientations. This paper is one of the first detailed studies of a skew scheme in which the axis directions after refinement do not either lie along or bisect those before. It raises the issue of how the analysis techniques can be applied in this new context and provides an example of how they may be thus applied.

1 Introduction

The possibility of a $\sqrt{5}$ scheme for subdivision surfaces was first discussed in [12]. There, two $\sqrt{5}$ mesh refinement rules for regular quadrilateral meshes were proposed, classified as $QP(2,1)$ and $QP(1,2)$, respectively. These two regular refinement rules, shown in Fig. 1(left), like the well-known $\sqrt{3}$ refinement rule for triangle meshes [17], induce a rotation of the initial mesh. In particular, the $QP(2,1)$ refinement induces an anti-clockwise rotation by $\arctan(\frac{1}{2})$, or equivalently a clockwise rotation by $\arctan(2)$, while the $QP(1,2)$ induces an anti-clockwise rotation by $\arctan(2)$, or equivalently a clockwise rotation by $\arctan(\frac{1}{2})$.

1.1 Related Work

Skew subdivision schemes, inducing a rotation of the grid at each iteration, were first introduced as a general class of subdivision schemes in [1]. $\sqrt{5}$ refinement was proposed in [23] as a hierarchical sampling method over a regular grid. In [22], a single step of the $\sqrt{5}$ refinement rule is described as a popular sampling method for numerical integration of two-dimensional periodic functions. In both applications the nice properties of the $\sqrt{5}$ sampling are due to fact that the five points corresponding to a square of the old grid (one old point and four new) all have different x and y coordinates, see Fig. 1(right).

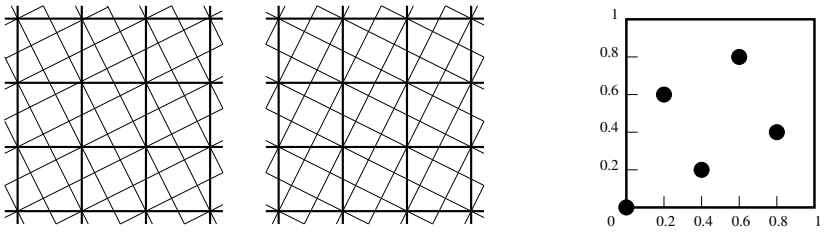

Fig. 1. Left: $QP(2,1)$ and $QP(1,2)$ refinement. Right: The five points corresponding to the same old quad have distinct x and y coordinates.

1.2 Overview

We propose a new subdivision scheme for quadrilateral meshes, based on the $\sqrt{5}$ refinement of a regular grid. In Sect. 2 we extend the refinement rule into irregular meshes, introducing the idea of using half-edges as the main primitive in the description of a subdivision scheme. In Sect. 3 we study the smoothness properties the $\sqrt{5}$ subdivision, tune its coefficients, and briefly discuss its support. We conclude by showing several examples of $\sqrt{5}$ subdivision surfaces.

2 $\sqrt{5}$-refinement for Irregular Meshes.

To define a $\sqrt{5}$ subdivision scheme, first, we need an extension of the regular refinement rules shown in Fig. 1 to cover the irregular case. Despite the fact that the regular case is already relatively complicated, it turns out that there is a very simple such extension, based in the correspondence between the vertices of the new mesh and the vertices and half-edges of the old.

Fig. 2 (left) shows the correspondence between the newly introduced vertices and the half-edges of the old mesh. As, at every step of the process, we retain the old vertices, we have a correspondence between the vertices of the new mesh and the vertices and half-edges of the old. A new vertex will be called *vertex-vertex* or *halfedge-vertex* according to this correspondence.

Under the same correspondence, the faces of the new mesh can be described as 4-tuples of vertices and half-edges of the old mesh. As Fig. 2 (right) shows, there are two kind of faces on the new mesh. Those corresponding to the faces of the old mesh, and those corresponding to the half-edges of the old mesh. Fig. 3 describes the new faces in terms of the old vertices and half-edges.

Notice that descriptions of subdivision processes using half-edges as the main primitive are not common in the literature. Probably, one reason is that half-edges, lacking a direct physical interpretation, are considered an unnatural choice, and a second reason is that subdivision schemes requiring the half-edge description, like the $\sqrt{5}$ scheme proposed here, have not been studied extensively. Nevertheless, the implementation of a scheme usually involves

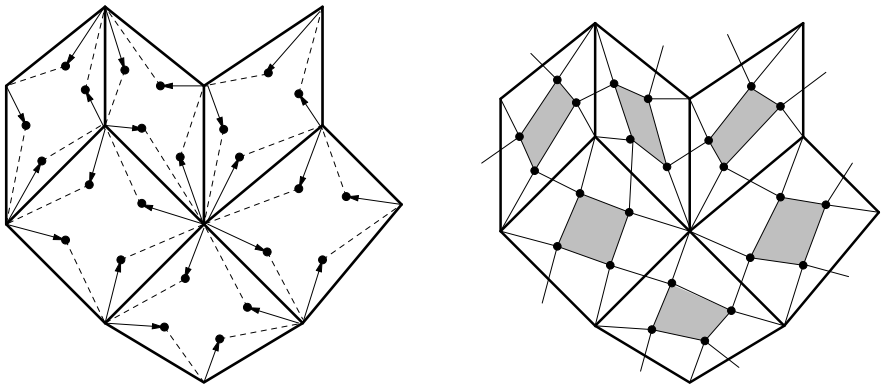

Fig. 2. Left: Every new vertex corresponds to an old half-edge. A solid and a dashed line connect the new vertex with the beginning and the end, respectively, of the corresponding old half-edge. Right: The shaded new faces correspond to old faces, the white new faces correspond to old half-edges.

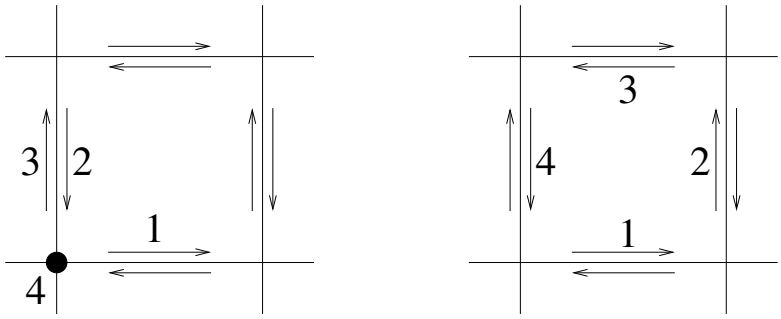

Fig. 3. Left: A new face corresponding to an old half-edge described as a 4-tuple (1,2,3,4) of old vertices and half-edges. Right: A new face corresponding to an old face described as a 4-tuple of old half-edges.

an implicit half-edge description, given that the most common computer representation for meshes is the Half-Edge structure. A generalisation of this idea is presented in the Appendix at the end of the paper.

3 Stencils for the $\sqrt{5}$-scheme.

The next step towards a definition of a subdivision scheme is to determine the point-sets of the *stencils*, that is, the set of old vertices that will be used for the calculation of the position of the new. A larger point-set, after correct tuning of the coefficients, gives smoother subdivision surfaces, while a smaller point set gives smaller support with the influence of each initial vertex better

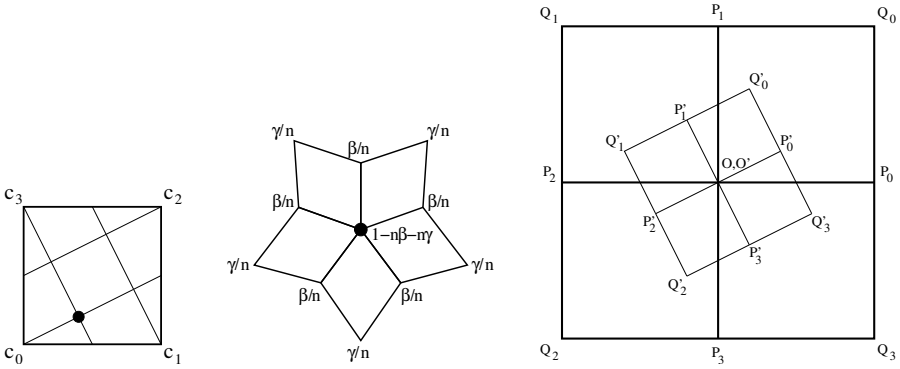

Fig. 4. Left: The stencil of the half-edge vertices. Middle: The stencil for the vertex vertices. Right: The transformation of the 1-ring of the vertex O.

localised. Here, we opt for small stencils and we use the vertices of the face of a half-edge for the stencil of the corresponding halfedge-vertex. For a vertex-vertex we use the corresponding old vertex and the members of its 1-ring neighbourhood, see Fig. 4.

Next we tune the coefficients in the stencils so that the resulting subdivision surfaces are as smooth as possible.

3.1 Background

Traditionally, there are two major tools for analysing the smoothness properties of a subdivision surface. The generating functions [9], and the spectral analysis of the subdivision matrix [8, 3, 20]. Here we use a version of spectral analysis with a more geometric flavor in the form of eigenpolygons [14, 16]. Although our analysis is elementary it is worth going into some detail, especially because the study of schemes with complex subdominant eigenvalues is scattered in the literature of subdivision.

Recall from [7] that the eigenvalues of the n-dimensional circulant matrix

$$C = circ(c_0, c_1, \ldots, c_{n-1}) = \begin{pmatrix} c_0 & c_1 & c_2 & \ldots & c_{n-2} & c_{n-1} \\ c_{n-1} & c_0 & c_1 & \ldots & c_{n-3} & c_{n-2} \\ & & & \ldots & & \\ c_2 & c_3 & c_4 & \ldots & c_0 & c_1 \\ c_1 & c_2 & c_3 & \ldots & c_{n-1} & c_0 \end{pmatrix} \tag{1}$$

are the values of the generating polynomial

$$\lambda_t = p(\omega^t), \qquad p(z) = c_0 + c_1 z + c_2 z^2 + \cdots + c_{n-1} z^{n-1}, \qquad \omega = e^{\frac{2\pi i}{n}} \tag{2}$$

for $t = 0, 1, \ldots, n-1$. The corresponding eigenvectors are given by the rows of the matrix

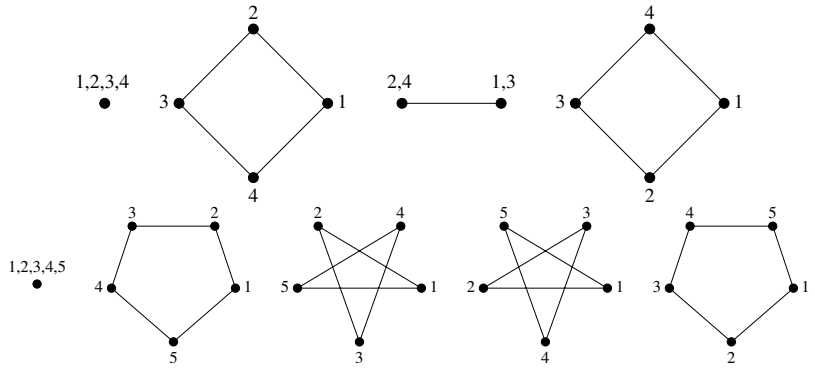

Fig. 5. The four eigenquadrilaterals and the five eigenpentagons.

$$F = \begin{pmatrix} 1 & 1 & 1 & \dots & 1 \\ 1 & \omega & \omega^2 & \dots & \omega^{n-1} \\ 1 & \omega^2 & \omega^4 & \dots & \omega^{2(n-1)} \\ \vdots & \vdots & \vdots & & \vdots \\ 1 & \omega^{n-1} & \omega^{2(n-1)} & \dots & \omega^{(n-1)(n-1)} \end{pmatrix} = (\mathbf{w_0}, \mathbf{w_1}, \mathbf{w_2}, \dots, \mathbf{w_{n-1}})^T. \quad (3)$$

These eigenvectors can also be seen as vertices of planar regular polygons, allowing multiple vertices and self-intersections. Fig. 5 shows these eigenpolygons for the cases $n = 4, 5$, while a detailed study of them can be found in [2].

Every planar polygon, thought of here as an n-tuple of coplanar points, or equivalently, an n-dimensional complex vector, can be uniquely written as a linear combination of the n eigenpolygons. A non-planar polygon can be written as a linear combination of the eigenpolygons, with the additional property that any two eigenpolygons corresponding to conjugate eigenvalues, i.e.

$$\mathbf{w_k}, \mathbf{w_{n-k}}, \quad k = 1, 2, \dots, \left\lfloor \frac{n}{2} \right\rfloor \quad (4)$$

lie on the same plane. The planes where the pairs of eigenpolygons lie can be computed by solving a linear system, see [5] for the details.

3.2 Analysis Around a Centreface

A very distinct property of the $\sqrt{5}$ scheme is that it is both primal and dual [12]. That is, one iteration of the subdivision process maps faces to faces and vertices to vertices. This also means that we have to study the behaviour of the scheme both around centrefaces and around vertices.

In the study of the behaviour of the scheme around a centreface we assume that all the faces are quadrilateral and thus, at each step, they are

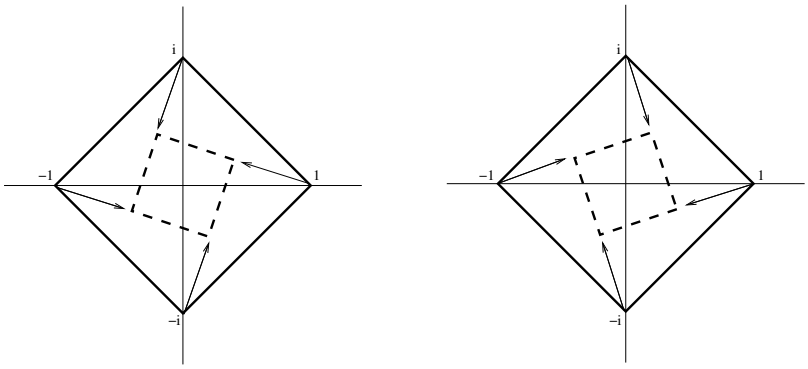

Fig. 6. The two convex eigenquads after one iteration of the $QP(2,1)$ subdivision. The result can be described as multiplication by $\frac{2}{5} + i\frac{1}{5}$ and $\frac{2}{5} - i\frac{1}{5}$, respectively.

transformed by a circulant matrix of dimension $n = 4$. By evaluating the generating polynomial at 1,i,-1,$-i$ we get the system

$$\begin{aligned} c_0 + c_1 + c_2 + c_3 &= 1 \\ c_0 + ic_1 - c_2 - ic_3 &= \lambda_1 \\ c_0 - c_1 + c_2 - c_3 &= \lambda_2 \\ c_0 - ic_1 - c_2 + ic_3 &= \lambda_3 \end{aligned} \tag{5}$$

To find the exact values of λ_1, λ_3 we notice that the transformation of the eigenpolygon $\mathbf{w_1}$ by one step of the subdivision scheme corresponds to a multiplication by

$$z = re^{i\theta} = \frac{2}{5} + i\frac{1}{5} \tag{6}$$

where r is the scaling and θ the rotation induced by the scheme. Similarly, the transformation on $\mathbf{w_3}$, which is a copy of $\mathbf{w_1}$ with opposite orientation, corresponds to a multiplication by

$$\bar{z} = re^{-i\theta} = \frac{2}{5} - i\frac{1}{5}. \tag{7}$$

But as $\mathbf{w_1}, \mathbf{w_3}$ are eigenpolygons their transformation is also equal to a multiplication by the corresponding eigenvalue. Thus, we have $\lambda_1 = \frac{2}{5} + i\frac{1}{5}$ and $\lambda_3 = \frac{2}{5} - i\frac{1}{5}$ (see Fig. 6).

In subdivision, the standard requirement for the fourth, fifth, and sixth eigenvalues is to depend quadratically on the two subdominant eigenvalues [21]. Indeed, as the two subdominant eigenvalues represent the transformation within the tangent plane, for nice curvature behaviour we would expect the dominant eigencomponents outside the tangent plane to shrink with a speed depending quadratically on the shrinkage of the tangent plane.

Thus, in our case, a natural choice for the fourth eigenvalue, which by the third equation of the system (5) is real, would be $\lambda_2 = |\lambda_1|^2 = |\lambda_3|^2 = \frac{1}{5}$. That leads to the coefficients

$$c_0 = \frac{5}{10} \quad c_1 = \frac{3}{10} \quad c_2 = \frac{1}{10} \quad c_3 = \frac{1}{10} \tag{8}$$

Notice that, with the above coefficients, points at different distances from the new point have the same influence on it.

Although in the rest of the paper we use the above coefficients, we have also examined other possibilities. The coefficients $\frac{12}{25}, \frac{8}{25}, \frac{2}{25}, \frac{3}{25}$, were obtained as Wachspress coordinates of the point $(\frac{2}{5}, \frac{1}{5})$ with respect to the unit square, see for example [11]. Another alternative is to use the coefficients $\frac{9}{20}, \frac{7}{20}, \frac{1}{20}, \frac{3}{20}$, which give $\lambda_2 = 0$ meaning that any new face corresponding to an old face is planar, because the only eigencomponent which possibly lies outside the tangent plane becomes 0. Finally, the coefficients $\frac{2}{5}, \frac{2}{5}, 0, \frac{1}{5}$, give $\lambda_2 = -\frac{1}{5}$.

Experimentally, we found that for $\lambda_2 = \frac{3}{25}$ we get visual results similar to those for $\lambda_2 = \frac{1}{5}$. For $\lambda_2 = 0$ the visual quality deteriorates slightly, while for $\lambda_2 = -\frac{1}{5}$ it is significantly worse, see Fig. 7. The latter shows that the behaviour of the scheme depends on the actual eigenvalues and not on their absolute values.

3.3 Analysis Around a Vertex

To study the smoothness properties of a surface around a vertex of valence n we consider the subdivision matrix

$$M = \begin{pmatrix}
1-\beta-\gamma & \frac{\beta}{n} & \frac{\gamma}{n} & \frac{\beta}{n} & \frac{\gamma}{n} & \frac{\beta}{n} & \frac{\gamma}{n} & \dots & \frac{\beta}{n} & \frac{\gamma}{n} \\
c_0 & c_1 & c_2 & c_3 & 0 & 0 & 0 & \dots & 0 & 0 \\
c_1 & c_2 & c_3 & c_0 & 0 & 0 & 0 & \dots & 0 & 0 \\
c_0 & 0 & 0 & c_1 & c_2 & c_3 & 0 & \dots & 0 & 0 \\
c_1 & 0 & 0 & c_2 & c_3 & c_0 & 0 & \dots & 0 & 0 \\
 & & & & & & & & & \\
 & & & & & & & & & \\
c_0 & c_3 & 0 & 0 & 0 & 0 & 0 & \dots & c_1 & c_2 \\
c_1 & c_0 & 0 & 0 & 0 & 0 & 0 & \dots & c_2 & c_3
\end{pmatrix} \tag{9}$$

acting on the vector

$$V = (O, P_0, Q_0, P_1, Q_1, \dots, P_{n-1}, Q_{n-1})^T \tag{10}$$

with O, P_i, Q_i as shown in Fig. 4 (right). As the c_i's are given by (8) we have to optimise for β and γ.

To streamline the computations we calculate the two eigenvalues corresponding to each frequency separately, see [4]. Apart from the obvious eigenvalue 1, we will call *elliptic* the two eigenvalues corresponding to frequency 0

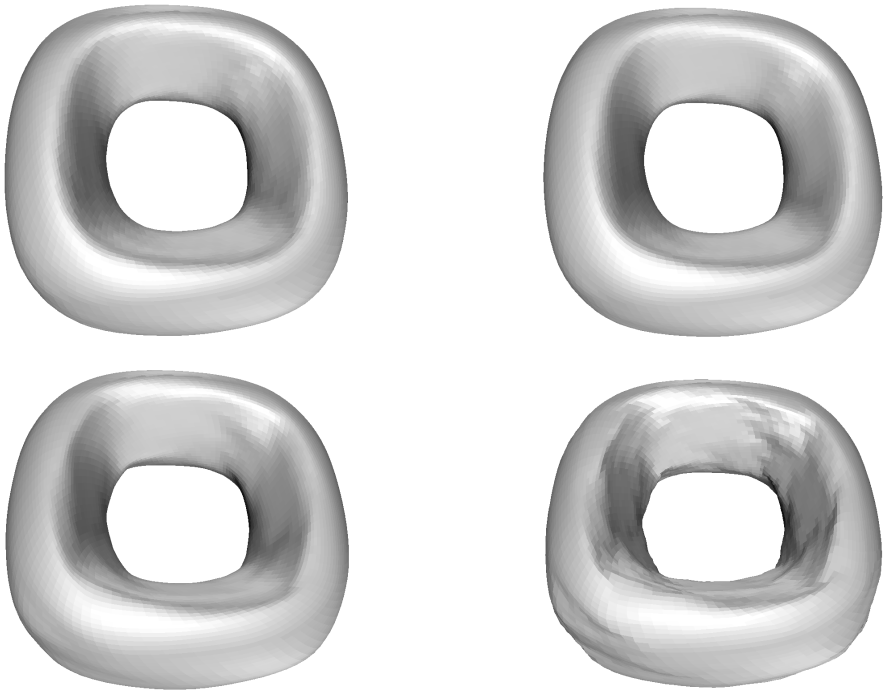

Fig. 7. Top left: $\lambda_2 = \frac{1}{5}$, top right: $\lambda_2 = \frac{3}{25}$, bottom left: $\lambda_2 = 0$, bottom right: $\lambda_2 = -\frac{1}{5}$.

because they are responsible for the elliptic properties of the scheme, and the remaining $2n-2$ eigenvalues *non-elliptic*.

We notice that β, γ seen here as variables, affect only the two elliptic eigenvalues, see for example [16]. Using this observation we prove in two stages that our scheme gives C^1 surfaces for generic input meshes. First we show that the largest eigenvalues λ_1, λ_{n-1} correspond to frequencies 1 and $n-1$, and all the other non-elliptic eigenvalues have smaller norm. Secondly we compute β, γ such that the elliptic eigenvalues are equal to $|\lambda_1|^2$ and 0.

The Non-elliptic Eigenvalues

The two non-elliptic eigenvalues corresponding to frequency j are given by the eigenvalues of the matrix

$$\begin{pmatrix} \lambda_j^p & c_2 \\ \lambda_j^q & c_3 \end{pmatrix} \tag{11}$$

where λ_j^p, λ_j^q are the jth eigenvalues of

$$C^p = circ(c_1, c_3, 0, \ldots, 0) = circ\left(\frac{3}{10}, \frac{1}{10}, 0, \ldots, 0\right) \tag{12}$$

and

$$C^q = circ(c_2, c_0, 0, \ldots, 0) = circ\left(\frac{1}{10}, \frac{5}{10}, 0, \ldots, 0\right) \tag{13}$$

respectively. For a geometric interpretation of the above we use a special decomposition of the two n-gons

$$\mathbf{P} = (P_0, P_1, \ldots, P_{n-1}), \quad \mathbf{Q} = (Q_0, Q_1, \ldots, Q_{n-1}) \tag{14}$$

as linear combinations of eigenpolygons, coming in pairs $\mathbf{P_j}, \mathbf{Q_j}$ of parallel polygons with the same frequency j. Then, excluding the influence of O on them (which is a similarity), the subdivision process transforms them by

$$\begin{pmatrix} \mathbf{P'_j} \\ \mathbf{Q'_j} \end{pmatrix} = \begin{pmatrix} \lambda_j^p \; c_2 \\ \lambda_j^q \; c_3 \end{pmatrix} \begin{pmatrix} \mathbf{P_j} \\ \mathbf{Q_j} \end{pmatrix} \tag{15}$$

For the details on constructing such a decomposition see [16].

Substituting c_2, c_3 from (8) and using (2) to calculate λ_j^p, λ_j^q we find the characteristic polynomial of (11)

$$\begin{vmatrix} \frac{3}{10} + \frac{1}{10}\omega^j - x & \frac{1}{10} \\ \frac{1}{10} + \frac{5}{10}\omega^j & \frac{1}{10} - x \end{vmatrix} = \frac{2}{100} - \frac{4}{100}\omega^j - (\frac{4}{10} + \frac{1}{10}\omega^j)x + x^2 \tag{16}$$

with roots

$$\lambda_j = \frac{\frac{4}{10} + \frac{1}{10}\omega^j \pm \sqrt{\frac{8}{100} + \frac{24}{100}\omega^j + \frac{1}{100}\omega^{2j}}}{2} \tag{17}$$

From this we can verify that for every n, the eigenvalues with the largest norms correspond to $j = 1, n-1$.

For the regular case $n = 4$ in particular, we find that the two subdominant eigenvalues are $\frac{2}{5} \pm i\frac{1}{5}$ as expected. The fourth and fifth eigenvalues are $\frac{3}{20} \pm i\frac{\sqrt{15}}{20}$ which means that, even in the regular case, the scheme is not C^2. Nevertheless, as their norm is near to the square of the norm of the subdominant eigenvalues, the quadratic properties of the scheme are acceptable in practice.

Tuning the Elliptic Eigenvalues

The elliptic eigenvalues of the scheme can be found from the 3×3 matrix

$$\begin{pmatrix} 1-\beta-\gamma & \beta & \gamma \\ c_0 & c_1 + c_3 & c_2 \\ c_1 & c_0 + c_3 & c_2 \end{pmatrix} = \begin{pmatrix} 1-\beta-\gamma & \beta & \gamma \\ \frac{5}{10} & \frac{4}{10} & \frac{1}{10} \\ \frac{3}{10} & \frac{6}{10} & \frac{1}{10} \end{pmatrix} \tag{18}$$

see [4]. After adding the second and third columns to the first, and then subtracting the first row from the second and third, we find the characteristic polynomial to be

$$(1-x)\begin{vmatrix} \frac{4}{10}-\beta-x & \frac{1}{10}-\gamma \\ \frac{6}{10}-\beta & \frac{1}{10}-\gamma-x \end{vmatrix} \tag{19}$$

and the two elliptic eigenvalues are

$$\frac{\beta+\gamma-\frac{1}{2} \pm \sqrt{(\beta+\gamma-\frac{1}{2})^2+\frac{8}{100}-\frac{8}{10}\gamma}}{2} \tag{20}$$

We notice that even after putting the largest elliptic eigenvalue equal to $|\lambda_1|^2$ we still have a degree of freedom left. We use this extra freedom to make the smallest elliptic eigenvalue equal to zero. This is a good strategy because the tuning of the eigenvalues is done for the limit after infinitely many subdivision steps, and by making zero the eigenvalues with no rôle in the limit, we avoid unwanted artifacts in the intermediate steps. Solving the system we find

$$\beta = \frac{2}{5} - |\lambda_1|^2 \quad \gamma = \frac{1}{10} \tag{21}$$

For example, for $n = 4$ we have $|\lambda_1|^2 = \frac{1}{5}$ giving $\beta = \frac{1}{5}$. Notice that $\beta = \frac{1}{5}$ is not optimal for every n, because $|\lambda_1|$ is not equal to $\frac{1}{5}$ for every n. Fig. 8 shows the results of smoothing a valence 3 vertex with $\beta = \frac{1}{5}$ instead of the correct $\beta \simeq 0.2518$. The difference is small but noticeable.

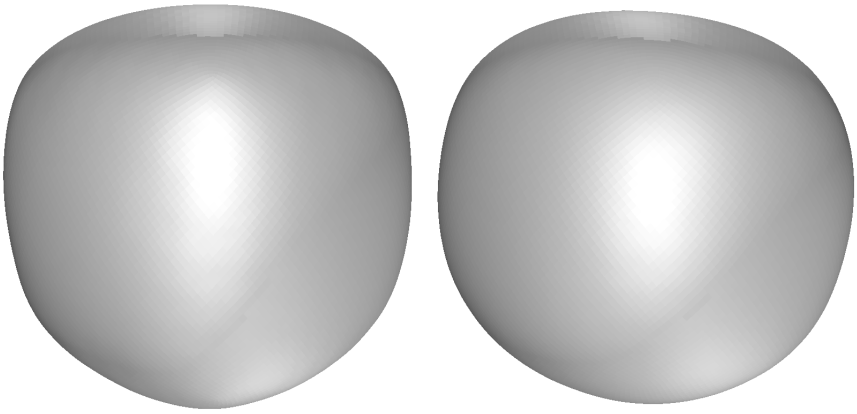

Fig. 8. Left: $\beta = 0.2$ for the valence 3 vertices. Right: $\beta = 0.2518$ for the valence 3 vertices.

3.4 The Support

After defining the stencils, the support of any $\sqrt{5}$ subdivision scheme depends only on the direction of the rotation of the grid at each step, that is, on the combination of steps of $QP(2,1)$ and $QP(1,2)$ we use. In the case we always keep the same direction for the rotation then the grid never aligns with the original grid and the support is fractal.

On the other hand, if we alternate the direction of the rotation at each step, then the grid aligns with the original every even number of iterations. In this case the *arity* of the double step is 5. Fig. 9 (left) shows the *footprint* of a double step, that is, the non-zero points of the basis function after a double step, and following [13] we can see that the support is again fractal. The same Figure also shows a polygonal subset of the support calculated with the method in [13]. Fig. 9 (right) shows an approximation of the support based on four iterations of the scheme.

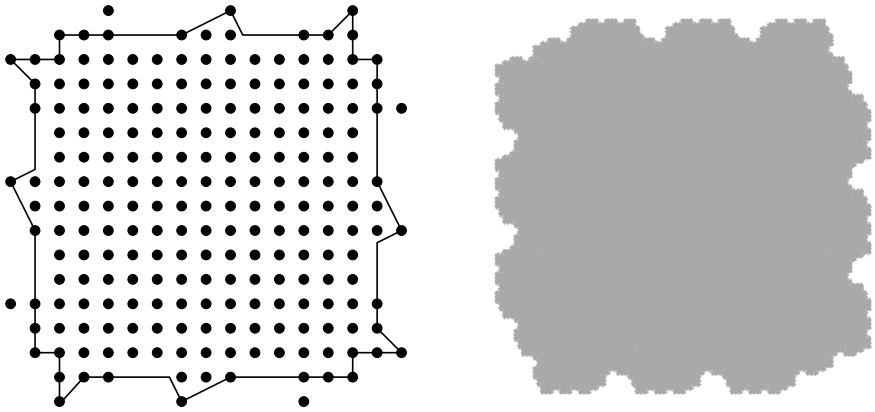

Fig. 9. Left: The footprint of the $\sqrt{5}$ scheme and a polygonal inner bound for the support, calculated using the method in [13]. Right: An approximation to the support based on four iterations of the scheme.

4 Results

We implemented the $\sqrt{5}$ scheme for quadrilateral meshes without boundaries. Due to the direct interpretation of the subdivision process in terms of half-edges, the code was less than three hundred lines, including the implementation of a half-edge structure. Fig. 10 shows some results.

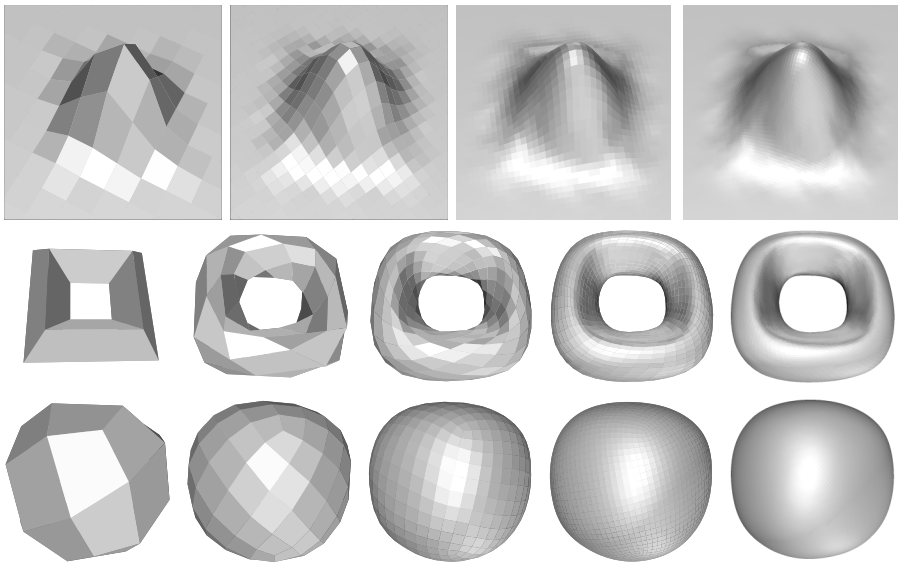

Fig. 10. First row: The basis function. Second row: A torus. Third row: A cube.

5 Conclusion – Future Work

We have presented a new $\sqrt{5}$ subdivision scheme for quad meshes. The most interesting aspects of this scheme are:

- The new points have unique x and y coordinates with respect to the old faces, giving room for fine-tuning with relatively small stencils.
- There is a natural correspondence between the new vertices and the old half-edges. That makes the implementation almost trivial, and leads to a general approach to subdivision as an averaging process with the half-edges as the main primitive.

The rotation of the grid at each subdivision step raises many questions on subdivision matrices with complex subdominant eigenvalues and, as we saw, the reduction of the problem to the case of real eigenvalues through norms, does not give satisfactory answers. In the future we plan a more systematic study of the fourth, fifth and sixth eigenvalues of a subdivision matrix when the second and the third eigenvalues are complex.

Acknowledgement

This work was supported in part by the European Union research project "Multiresolution in Geometric Modelling (MINGLE)" under grant HPRN–CT–1999–00117.

Appendix

The way we calculate a halfedge-vertex in the $\sqrt{5}$-scheme suggests a general averaging operator which can be used for a general description of subdivision. Let

$$(P_0, P_1, \ldots, P_{n-1})^T \tag{22}$$

be a face of the mesh consisting of n vertices, written here as a $n \times 1$ vector, and let

$$c_0 P_0 + c_1 P_1 + \cdots + c_{n-1} P_{n-1} \tag{23}$$

be a new point corresponding to the half-edge $\mathbf{P_0 P_1}$. Then, by the rotational symmetry of the connectivity of the face, all the new points corresponding to its half-edges are given by

$$C \times (P_0, P_1, \ldots, P_{n-1})^T \tag{24}$$

where C is a circulant matrix.

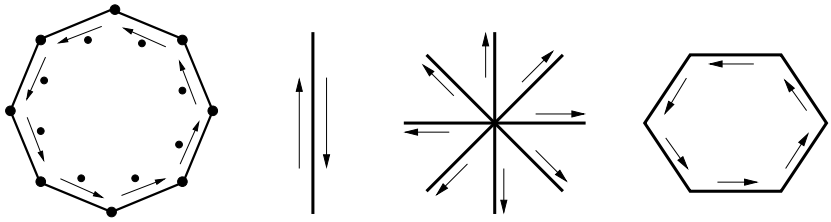

Fig. 11. (**a**) The circulant averaging operator $\mathcal{C}$. The small dots, each one corresponding to a half-edge of the face, are the new vertices (half-edge vertices). (**b**),(**c**),(**d**) The mean average of the halfedge-vertices corresponding to an old edge, vertex, or face, is used as a second operator.

Thus, the calculation of new points corresponding to old half-edges can be seen as the action on the mesh of a *circulant averaging operator* $\mathcal{C}$. Interestingly, many major approximating subdivision schemes can be described as the combination of $\mathcal{C}$ with the mean averaging of the halfedge-vertices corresponding to the same old edge, vertex, or face, see Fig. 11.

Below we give examples of well-known schemes described in this way:

- **Doo-Sabin:** Traditionally, the Doo-Sabin scheme is not described with the use of half-edges. However it has a trivial description in terms of the operator $\mathcal{C} = circ(\frac{9}{16}, \frac{3}{16}, \frac{1}{16}, \frac{3}{16})$.
- **Loop:** To describe the Loop [18] scheme for triangle meshes we use $\mathcal{C} = circ(\frac{3}{8}, \frac{1}{4}, \frac{3}{8})$. Then we calculate a vertex-vertex as a linear combination of the corresponding old vertex and the mean average of the points

corresponding to the half-edges starting from it, see Fig. 11(c). To find a mid-edge vertex we average the two points corresponding to the two half-edges of that edge, see Fig. 11(b).

- **Catmull-Clark:** Similarly, for the Catmull-Clark scheme we use $\mathcal{C} = circ(\frac{1}{8}, \frac{1}{8}, \frac{1}{8}, \frac{5}{8})$. We notice that for any vertex, averaging around all the faces adjacent to it gives six times as much weight to the vertices directly connected to it than to the vertex opposite to it, thus leading to the original coefficients proposed in [6].

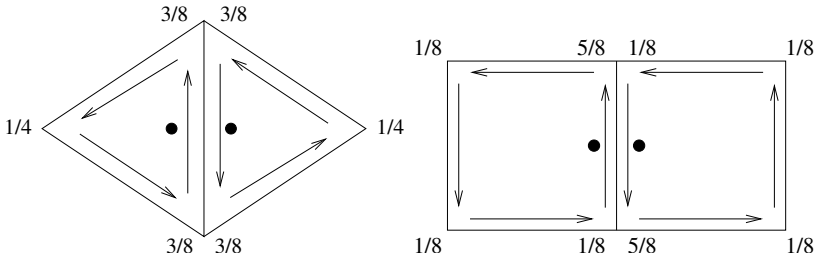

Fig. 12. Left: In the Loop scheme $\mathcal{C}$ acts with coefficients $(\frac{3}{8}, \frac{1}{4}, \frac{3}{8})$. Right: In the Catmull-Clark scheme C acts with coefficients $(\frac{1}{8}, \frac{5}{8}, \frac{1}{8}, \frac{1}{8})$.

The mean averaging operator has been extensively studied in the context of subdivision [10, 19, 15], and shown to have nice smoothness properties. But it also has serious limitations in describing the existing schemes with their usual stencils. Several extensions of the mean averaging operator have been proposed in [19], but, to the best of our knowledge the circulant averaging operator $\mathcal{C}$ has not been studied in full generality in the context of subdivision.

References

1. M. Alexa. Split operators for triangular refinement. *Computer Aided Geometric Design*, 19(3):169–172, 2002.
2. F. Bachmann and E. Schmidt. *n-Ecke*. B.I.-Hochschultaschenbücher, 1970.
3. A. A. Ball and D. J. T. Storry. Conditions for tangent plane continuity over recursively generated B-spline surfaces. *ACM Transactions on Graphics*, 7(2):83–102, 1988.
4. L. Barthe, C. Gérot, M. A. Sabin, and L. Kobbelt. Simple computation of the eigencomponents of a subdivision matrix in the Fourier domain. In N. A. Dodgson, M. S. Floater, and M. A. Sabin, editors, *Advances in Multiresolution for Geometric Modelling*, pages 245–257 (this book). Springer, 2004.
5. E. R. Berlekamp, E. N. Gilbert, and F. W. Sinden. A polygon problem. *Am. Math. Mon.*, 72:233–241, 1965.
6. E. Catmull and J. Clark. Recursively generated B-spline surfaces on arbitrary topological meshes. *Computer-Aided Design*, 10:350–355, 1978.

7. P. J. Davis. *Circulant matrices*. Chichester: Wiley, New York, 1979.
8. D. Doo and M. Sabin. Behaviour of recursive division surfaces near extraordinary points. *Computer-Aided Design*, 10:356–360, 1978.
9. N. Dyn. Subdivision schemes in computer-aided geometric design. In W. Light, editor, *Advances in Numerical Analysis*, volume 2, pages 36–104. Clarendon Press, 1992.
10. N. Dyn, D. Levin, and J. Simoens. Face value subdivision schemes on triangulations by repeated averaging. In A. Cohen, J.-L. Merrien, and L. L. Schumaker, editors, *Curve and Surface Fitting: Saint-Malo 2002*, pages 129–138. Nashboro Press, 2003.
11. M. S. Floater. Mean value coordinates. *Computer Aided Geometric Design*, 20(1):19–28, 2003.
12. I. P. Ivrissimtzis, N. A. Dodgson, and M. A. Sabin. A generative classification of mesh refinement rules with lattice transformations. *Computer Aided Geometric Design*, 21(1):99–109, 2004.
13. I. P. Ivrissimtzis, M. A. Sabin, and N. A. Dodgson. On the support of recursive subdivision. *ACM Transactions on Graphics*. To appear.
14. I. P. Ivrissimtzis and H.-P. Seidel. Evolutions of polygons in the study of subdivision surfaces. *Computing*. To appear.
15. I. P. Ivrissimtzis, K. Shrivastava, and H.-P. Seidel. Subdivision rules for general meshes. In A. Cohen, J.-L. Merrien, and L. L. Schumaker, editors, *Curve and Surface Fitting: Saint-Malo 2002*, pages 229–238. Nashboro Press, 2003.
16. I. P. Ivrissimtzis, R. Zayer, and H.-P. Seidel. Polygonal decomposition of the 1-ring neighborhood of the Catmull-Clark scheme. In *Proc. Shape Modeling International*, 2004. To appear.
17. L. Kobbelt. $\sqrt{3}$ subdivision. In *Proc. ACM SIGGRAPH 2000*, pages 103–112, 2000.
18. C. T. Loop. Smooth subdivision surfaces based on triangles. Master's thesis, University of Utah, Department of Mathematics, 1987.
19. P. Oswald and P. Schröder. Composite primal/dual sqrt(3)-subdivision schemes. *Computer Aided Geometric Design*, 20(3):135–164, 2003.
20. U. Reif. A unified approach to subdivision algorithms near extraordinary vertices. *Computer Aided Geometric Design*, 12(2):153–174, 1995.
21. M. A. Sabin. Eigenanalysis and artifacts of subdivision curves and surfaces. In A. Iske, E. Quak, and M. S. Floater, editors, *Tutorials on Multiresolution in Geometric Modelling*, pages 69–92. Springer, 2002.
22. I. H. Sloan and S. Joe. *Lattice methods for multiple integration*. Oxford Science Publications. Oxford: Clarendon Press., 1994.
23. M. Stamminger and G. Drettakis. Interactive sampling and rendering for complex and procedural geometry. In *Proc. Eurographics Workshop on Rendering*, pages 151–162, 2001.